minerals

MDPI

Article

Geophysical Properties of Precambrian Igneous Rocks in the Gwanin Vanadiferous Titanomagnetite Deposit, Korea

Seungwook Shin, Seongjun Cho *, Euijun Kim and Jihyun Lee

Korea Institute of Geoscience and Mineral Resources, 124 Gwahak-ro, Yuseong-gu, Daejeon 34132, Korea; sw.shin@kigam.re.kr (S.S.); euijun.kim@kigam.re.kr (E.K.); jihyun.lee@kigam.re.kr (J.L.)
* Correspondence: mac@kigam.re.kr

Abstract: Precambrian igneous rocks (851–873 Ma) occur in Pocheon City, Korea. These rocks—crystallized during magmatic differentiation—formed vanadiferous titanomagnetite (VTM) deposit. Vanadium is a crucial element in vanadium redox flow batteries that are most appropriate for large-scale energy storage systems. We investigated the VTM deposit to evaluate its size and the possible presence of a hidden orebody. We demonstrated laboratory experiments of density, susceptibility, resistivity, and chargeability of the Precambrian igneous rocks to enhance the interpretation accuracy of geophysical surveys. The rocks consisting of underground ore (UO), discovered ore (DO), gabbro (GA), monzodiorite (MD), and quartz monzodiorite (QMD) were sampled from drilling cores and outcrops. The average density values were UO: 4.57 g/cm^3, DO: 3.63 g/cm^3, GA: 3.26 g/cm^3, MD: 3.18 g/cm^3, and QMD: 2.85 g/cm^3. The average susceptibility values were UO: 0.8175 SI, DO: 0.2317 SI, GA: 0.0780, MD: 0.0126 SI, and QMD: 0.0007. The average resistivity values were UO: 2 Ωm, DO: 36 Ωm, GA: 257 Ωm, MD: 4571Ωm, and QMD: 7801 Ωm. The chargeability values were UO: 143 mV/V, DO: 108 mV/V, GA: 79 mV/V, MD: 42 mV/V, and QMD: 9 mV/V. We found that the properties of the mineralized rocks are considerably different from those of the surrounding rocks. This result may facilitate the mineral exploration of VTM deposits.

Keywords: Precambrian igneous rock; geophysical property; laboratory measurement

check for updates

Citation: Shin, S.; Cho, S.; Kim, E.; Lee, J. Geophysical Properties of Precambrian Igneous Rocks in the Gwanin Vanadiferous Titanomagnetite Deposit, Korea. *Minerals* **2021**, *11*, 1031. https://doi.org/10.3390/min11101031

Academic Editor: Michael S. Zhdanov

Received: 12 August 2021
Accepted: 17 September 2021
Published: 23 September 2021

Publisher's Note: MDPI stays neutral with regard to jurisdictional claims in published maps and institutional affiliations.

Copyright: © 2021 by the authors. Licensee MDPI, Basel, Switzerland. This article is an open access article distributed under the terms and conditions of the Creative Commons Attribution (CC BY) license (https://creativecommons.org/licenses/by/4.0/).

1. Introduction

Precambrian igneous rocks—known as the Gonamsan intrusion—occur in the northwest part of Korea and were formed in ca. 851–873 Ma [1]. Vanadiferous titanomagnetite (VTM) deposits are mined in the Gonamsan intrusion. They represent a great source of vanadium, which is used in the production of alloys, ceramics, glasses, pigments, and vanadium redox flow batteries (VRBs) [2]. The latter, in particular, are suitable for large-scale energy storage systems (ESSs) [3]. The demand for VRBs is likely to increase in the future, given the commitments to the goals of global carbon neutrality [2]. A stable supply chain of vanadium can represent one of the most critical issues in terms of national industrial growth.

We have carried out research on VTM deposits since 2019, among which the Gonamsan intrusion was our first research site. Mineral exploration consists of geological mapping, geochemical and geophysical surveying, and drilling. The exploration strategy depends on both the exploration budget and objective [4]. We established a strategy for the VTM deposit and conducted geological mapping, geochemical surveys, aero-magnetic surveys, electrical resistivity tomography, and drilling [5,6]. We collected typical rocks of the Gonamsan intrusion from drilled cores and outcrops.

The quality of geophysical modeling, geology differentiation, and machine-learning-based prediction of potential orebodies can be improved by constructing a rich dataset of geophysical properties. To this end, we performed an extensive investigation to characterize the rock density, susceptibility, resistivity, and chargeability, which were associated

to gravity surveys, magnetic surveys, electrical resistivity tomography/electromagnetic surveys, and induced polarization surveys, respectively.

2. Materials and Methods

We generated a three-dimensional (3D) geological model of the area in the Gonamsan intrusion to understand both the geologic and topographic characteristics. The modeling was based on KIGAM's geologic map of Korea at a scale of 1:50,000 [7]. The simulations were performed using Paradigm SKUA-GOCAD 19. Figure 1 shows the generated 3D geological model with a location map of the survey site.

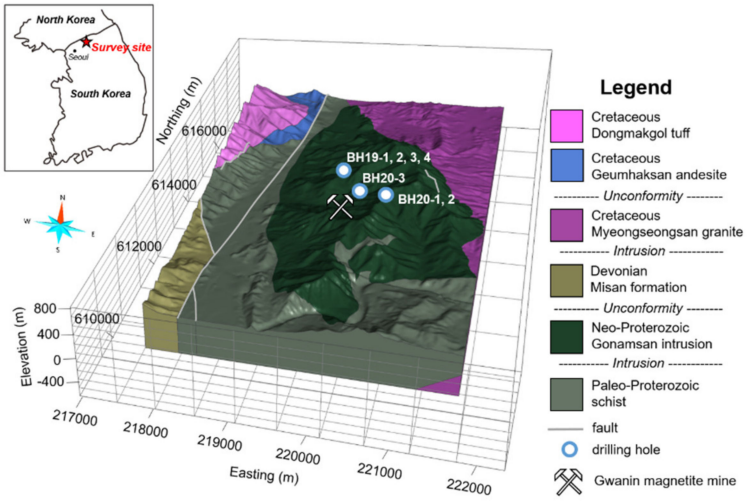

Figure 1. Three-dimensional geologic model of the Gonamsan intrusion area.

2.1. Geology

Gonamsan intrusion is located in Pocheon (Korea), and this area consists of five geologic units (Figure 1). Paleo-Proterozoic schist (1.9 Ga) forms the basement rock where all age data of the rocks were obtained by SHRIMP zircon U-Pb analysis [7]. The schist is intruded by Neo-Proterozoic Gonamsan intrusion (851–873 Ma) [1]. The Gonamsan intrusion extends horizontally for 3 km in the north–south direction and 1.5 km in the east–west direction. The typical characteristics of magmatic differentiation in the Gonamsan intrusion were confirmed by the geologic mapping of outcrops/mine and petrography of drilling cores. The Gonamsan intrusion was divided into ore, oxide gabbro, monzodiorite-monzogabbro, and quartz monzodiorite [8]. Devonian Misan formation (447–337 Ma), consisting of metamorphic sedimentary rocks, occurs southwest of the Precambrian schist. Cretaceous Myeongseongsan granite (110–114 Ma) is in contact with the northeast face of the Gonamsan intrusion. Cretaceous Geumhaksan andesite and Cretaceous Dongmgkgol tuff were formed via volcanism northwest of the Precambrian schist. North northeast (NNE)—south southwest (SSW) and north northwest (NNW—south southeast (SSE) striking faults were observed in this area.

Stratiform and lens-shaped VTM ores were observed in the Gonamsan intrusion. It was suggested that the VTM ores were mineralized by fractional crystallization of the mafic magma forming the intrusion, where stratiform and lens-shaped ores are located in both its lower and upper zones [8]. Underground mining of the Gwanin magnetite mine produces iron and titanium concentrates from high-grade stratiform ore, and a separation technique is being developed for vanadium.

2.2. Rock Samples

Figure 2 shows the rock samples collected from the underground ores and drilling cores in the Gonamsan intrusion to retrieve geophysical properties under laboratory conditions. Since the Gonamsan intrusion consists of mafic rocks, we classified the rock types by

petrography based on the ratio of mafic minerals to felsic minerals related to magmatic differentiation. Compared to other rocks, the VTM ores exhibited strong magnetism when examined using magnets. We collected samples of representative rock types consisting of underground ore (UO, 55 samples), discovered ore (DO, 55 samples), gabbro (GA, 40 samples), monzodiorite (MD, 49 samples), and quartz monzodiorite (QMD, 60 samples). DO was newly discovered in our study using both an aero-magnetic survey and drilling in 2020 [5].

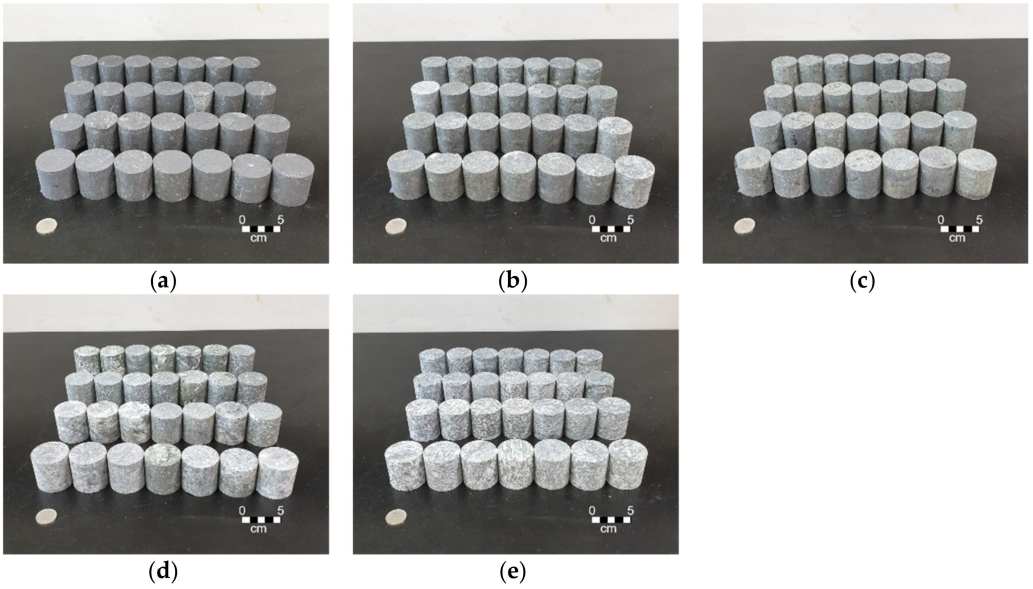

Figure 2. Rock samples of the Gonamsan intrusion for laboratory experiments: (**a**) underground ore, (**b**) discovered ore, (**c**) gabbro, (**d**) monzodiorite, and (**e**) quartz monzodiorite.

The mafic minerals in UO, DO, and GA were prominently abundant compared to those in MD and QMD. Moreover, the proportion of mafic minerals in MD was higher than that in QMD. UO and DO exhibit strong magnetism, differently from GA, MD, and QMD.

2.3. Laboratory Measurement System

Figure 3 illustrates the laboratory measurement system. Geophysical properties (density, susceptibility, resistivity, and chargeability) were evaluated to understand the geophysical characteristic of the rocks. Such understanding is required for geophysical interpretation and geology differentiation from field geophysical survey data.

Magnetite is the most abundant among the VTM ores, and its geophysical properties are distinct compared to those of silicates [9]. Knowledge of these properties is, thus, useful for determining the boundaries between the potential orebody and the host rocks using gravity, magnetic, electrical resistivity tomography, and induced polarization surveys carried out in the field. Rock density, defined as mass per unit volume, depends on the specific gravities of the main minerals and pores and is estimated by the buoyancy method using information on both the dehydrated grain mass and water-saturated mass. The dry density (D_{dry}; g/cm^3) was estimated as [10]:

$$D_{dry} = \frac{M_s}{M_{sat} - M_s} \quad (1)$$

where M_s is the dehydrated grain mass (g), and M_{sat} is the water-saturated mass (g).

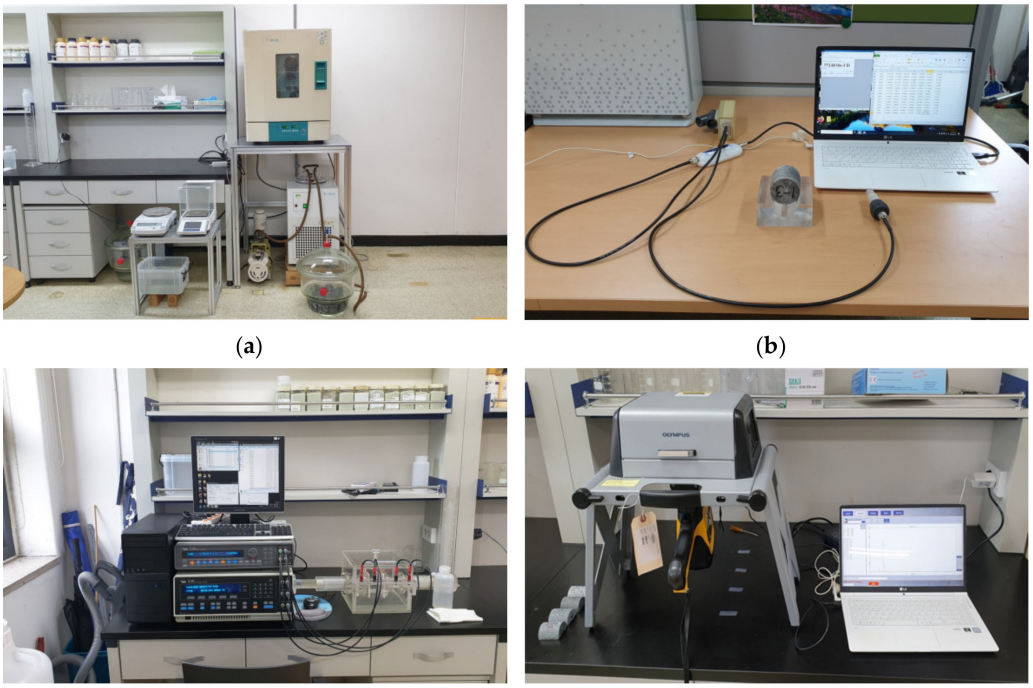

Figure 3. Laboratory measurement system for (**a**) density, (**b**) susceptibility, (**c**) resistivity/chargeability, and (**d**) X-ray fluorescence.

Figure 3a shows the density measurement system. The dehydrated grain mass was measured in air after dehydrating the rock samples in an oven at 110 °C for 24 h. The water-saturated mass was measured in the air after saturating the rock samples with a NaCl 0.001 M aqueous solution using a vacuum pump, in which the aqueous solution was injected in the rocks at a constant rate. The mass was measured using an electronic scale (±0.01 g).

The susceptibility (k, dimensionless), that is, the ratio of magnetization of the rocks to the magnetic field strength, is defined as:

$$k = \frac{M}{H} \tag{2}$$

where M indicates the magnetization (A/m), and H the magnetic field intensity (A/m).

As the magnetite in the VTM ores is ferromagnetic, magnetic surveying is the most important among the geophysical tools. The susceptibility of the rock samples was measured using a MS3 susceptibility meter, Bartington, Oxfordshire Withney, England and an MS2F field surface probe Bartington, Oxfordshire Withney, England, as shown in Figure 3b. The system is able to measure rock susceptibility up to 21 SI and has a resolution of 2×10^{-6} SI.

Resistivity (ρ) is an electrical property that describes the ability to impede electric current when direct current (DC) is injected into the rock. It mainly depends on the mineral types and porosity of the rock [11] and can be expressed as (Ωm):

$$\rho = R \times \frac{S}{L} \tag{3}$$

where R is the measured resistance while injecting DC (Ω), S is cross-section area of rock (m^2), and L is its length (m).

Chargeability (m) refers to the electric charge that remains at the interface between polarized minerals and pore water in rock after shutting off DC injection during a resistivity measurement. It is defined as (mV/V):

$$m = \frac{V_s}{V_p} \tag{4}$$

where V_s is the measured voltage after shutting off DC injection (V), and V_p is the measured voltage during DC injection (V).

Many metallic minerals are more electrically conductive and capacitive compared to gangue minerals [9,12]. A time-domain-induced polarization survey that acquires both resistivity and chargeability data is an effective tool for mineral exploration [13]. Resistivity and chargeability were measured using a SI 1287, Solartron metrology, West Sussex, England (Figure 3c).

Figure 3d demonstrates the X-ray fluorescence (XRF) analysis, which entailed the use of an Delta professional and an XRF portable workstation, Olympus, Tokyo, Japan. We selected five rock samples, representative of each rock type, to acquire and both the XRF data and their geophysical properties. We comprehensively characterized both types of data, as the characterization can improve our insights when conducting geophysical surveys of VTM deposits.

3. Results and Discussion

We characterized the geophysical properties of the rock samples by plotting histograms and calculating means and standard deviations. Figure 4 shows the results relative to density. The values for UO and DO were remarkably high compared to those of the other rock samples (Figure 4a,b). The average densities of UO and DO were 140% and 111% higher than those of GA, respectively. Ore minerals consisting of magnetite and ilmenite were abundant in UO and DO, as seen from Figure 2a,b. The specific gravity of the ore minerals is markedly higher than that of gangue minerals. Thus, the high density is caused by the presence of ore minerals in the rock samples. From this perspective, it is reasonable to suggest that the ore grade of UO was higher but more variable than that of DO given the higher mean and standard deviation of UO.

The average density of GA was higher than that of MD, as shown in Figure 4c,d. Moreover, Figure 4e illustrates that the mean QMD was the smallest among the rock samples. Mafic minerals (major) and the disseminated ore minerals (minor) were mainly observed in GA and MD (Figure 2c,d), whereas felsic minerals in QMD were the most abundant among the three types of rock samples (Figure 2e). The specific gravity of mafic minerals is higher than that of felsic minerals. The density variations of GA, MD, and QMD were associated with their magmatic differentiation. The standard deviation of the MD samples was the largest among the rock samples. This finding indicates that the mineral composition of MD is relatively distinct from that of the ore minerals to the felsic minerals compared to other rock samples. Therefore, we suggest that the gravity survey is effective in exploring the hidden VTM orebody and investigating the magmatic differentiation of the Gonamsan intrusion.

Figure 5 shows the histograms and statistics of susceptibility. The susceptibility of UO was the largest; the average susceptibilities of UO and DO were 1048% and 297% larger than that of GA, as displayed in Figure 5a–c. The susceptibility contrast between the UO and DO was more remarkable than the density contrast. The susceptibility ranges of DO and GA overlapped in Figure 5b,c, respectively. Figure 5b indicates that the standard deviation of DO is the highest. The content variation between DO was the largest of the rock samples because the susceptibility difference is sensitive to the content of magnetite (ferromagnetic minerals).

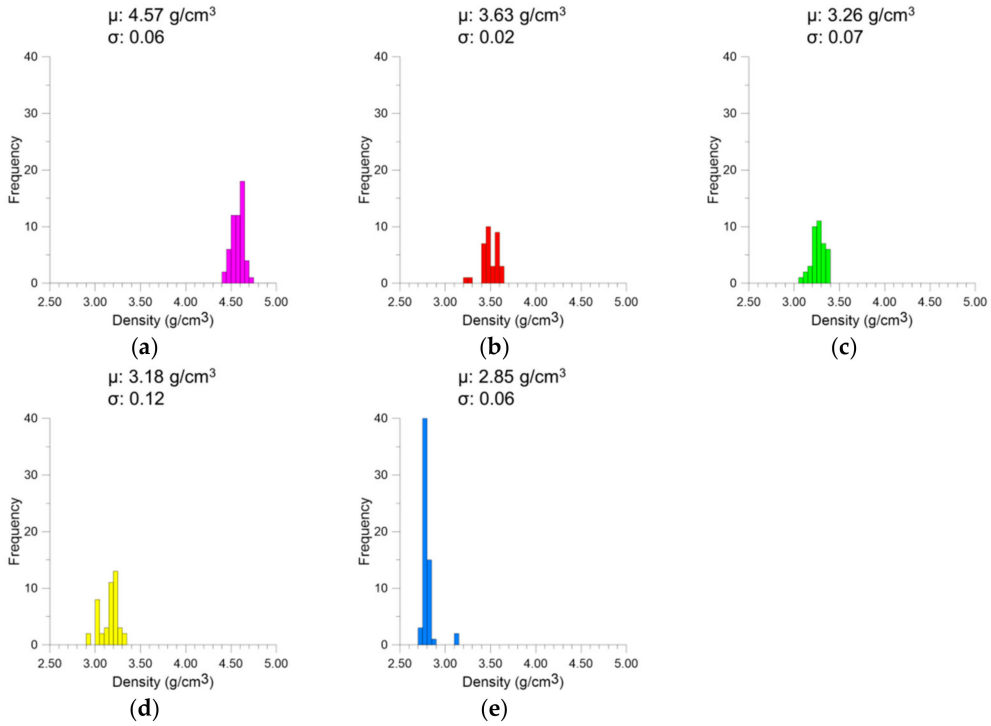

Figure 4. Histograms of density of rocks including mean (μ) and standard deviation (σ) of (**a**) underground ore, (**b**) discovered ore, (**c**) gabbro, (**d**) monzodiorite, and (**e**) quartz monzodiorite.

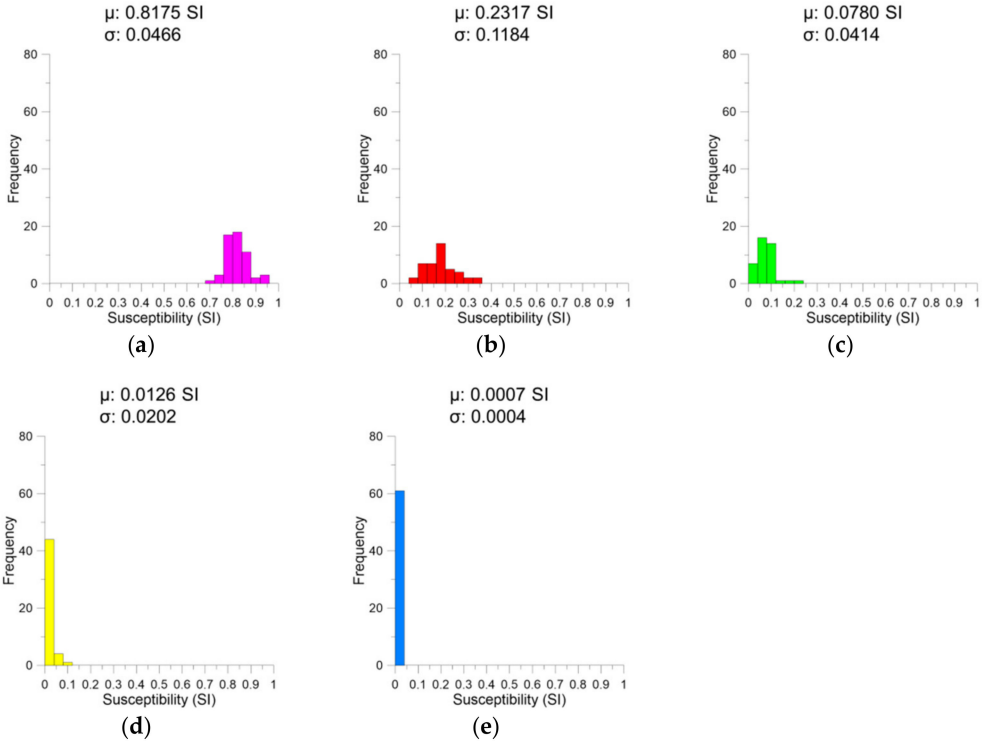

Figure 5. Histograms of susceptibility of rocks including mean (μ) and standard deviation (σ) of (**a**) underground ore, (**b**) discovered ore, (**c**) gabbro, (**d**) monzodiorite, and (**e**) quartz monzodiorite.

The average susceptibilities of GA and MD are 11,109% and 1791% larger than that of QMD, respectively (see Figure 5c–e). Although disseminated ore minerals were observed in several GA and MD samples (Figure 2c,d), ore minerals are extremely rare in QMD. Therefore, we suggest that the magnetic survey results imaging the subsurface susceptibility

differences are more effective than the gravity survey results for detecting the hidden VTM orebody.

The resistivity difference of the rocks was displayed using a logarithmic scale (Figure 6). The resistivity of UO and DO was relatively lower than that of GA (Figure 6a–c). In particular, the average resistivity and standard deviation of UO were the lowest, as seen from Figure 6a. The standard deviation of the UO was lower than that of the DO stemmed from the susceptibility results. The presence of ore minerals is a major factor that lowers the resistivity of rocks because ore minerals are good conductors.

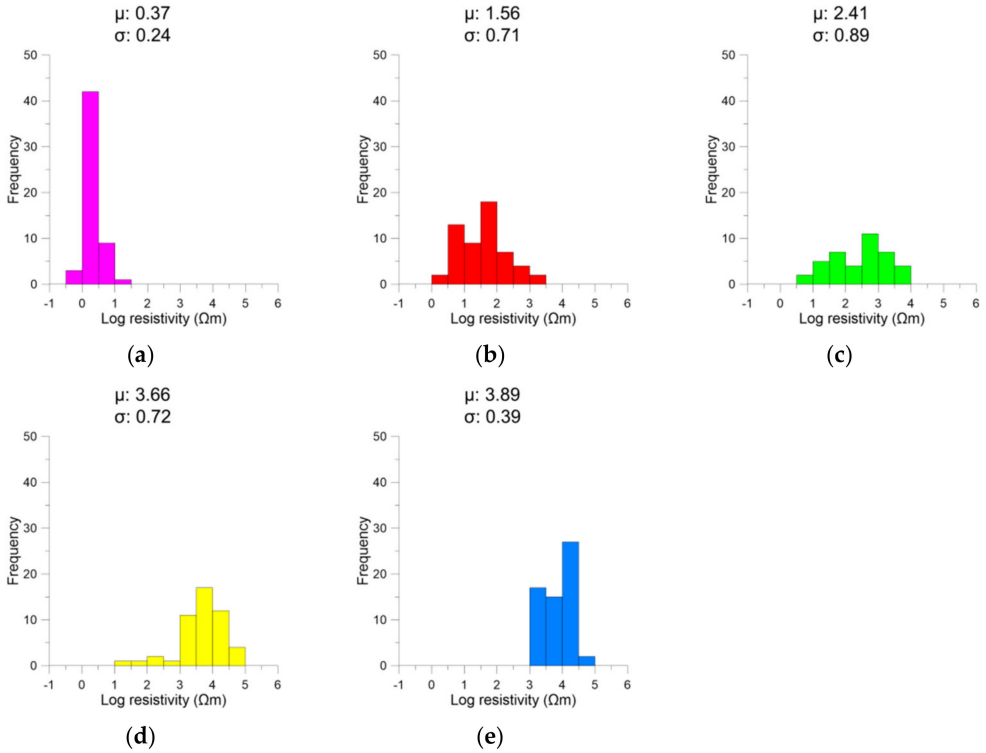

Figure 6. Histograms of logarithmic resistivity of rocks including mean (μ) and standard deviation (σ) of (**a**) underground ore, (**b**) discovered ore, (**c**) gabbro, (**d**) monzodiorite, and (**e**) quartz monzodiorite.

The resistivity of GA was lower than that of MD and QMD (Figure 6c–e). The two GA samples had a resistivity <10 Ωm. In the two samples, the ore mineral content was similar to that of UO or DO. The resistivities of MD and QMD were higher than those of the other rock samples, as illustrated in Figure 6d,e. Therefore, we surmise that rocks can be classified into ores and host rocks using a resistivity threshold of 10 Ωm.

Figure 7 displays the histograms and statistics of chargeability. The chargeability of UO was the largest among the rock samples, as shown in Figure 7a. The average chargeability of UO and DO was 181% and 136% larger than that of GA, respectively (see Figure 7a–c). In contrast, the chargeability between UO and DO was less remarkable than the other properties.

The chargeability of GA and MD was 870% and 461% larger than that of QMD, respectively (see Figure 7c–e). The patterns of this property were identical to those of other properties; however, the chargeability of the rock samples, except for QMD, overlapped in the range of 40 to 80 mV/V. Hence, we suggest that the chargeability facilitates the identification of ore minerals, but it is less sensitive to changes in the content of ore minerals.

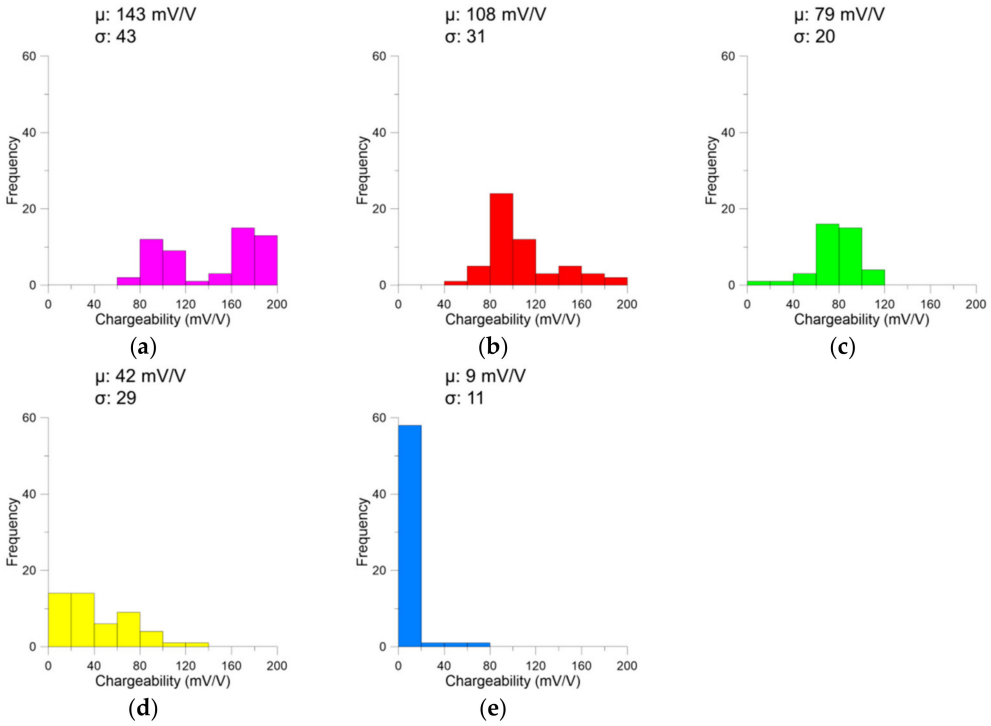

Figure 7. Histograms of chargeability of rocks including mean (μ) and standard deviation (σ) of (**a**) underground ore, (**b**) discovered ore, (**c**) gabbro, (**d**) monzodiorite, and (**e**) quartz monzodiorite.

Figure 8 shows rock slab images, potable XRF analysis results, and geophysical properties of the five kinds of rock samples (UO9, DO1-1, GA1, MD19-2, QMD3-3). The ore minerals were abundant in the rock slabs of UO9 and DO1-1 in which their metallic contents (Fe, Ti, and V) were higher than that in GA1 (Figure 8a–c). The ore minerals were disseminated in GA1 and MD19-2 but were not evidenced in QMD3-3, as seen from Figure 8c–e. Moreover, the metallic contents of GA1 and MD 19-2 were higher than that of QMD3-3.

The density and susceptibility of UO9 and DO1-1 were prominently higher than those of GA1 (Figure 8a–c). These patterns were identical to those of the electrical properties of UO9 and GA1. In addition, the patterns were in accordance with the results of GA1 and MD19-2 and with the results of QMD3-3 (Figure 8c–e). It is reasonable to suggest that the geophysical properties of the rocks in the Gonamsan intrusion were the most dependent on the ore mineral content. However, the resistivity and chargeability of DO1-1 were the same and were lower than those of GA1, respectively. It is necessary to further study the discordance between the chemical and electrical properties.

The densities of both magnetite and ilmenite are obviously different from those of major minerals in mafic intrusions [9]. Moreover, the magnetite is the most typical ferromagnetic material. The densities and susceptibility of UO were distributed within the properties ranges of magnetite ores in Bushveld deposit, South Africa and Taihe iron deposit, China [14,15]. The ranges of the properties of DO were inlcuded in those of titanomagnetite ores in New Zeleand [16]. Therefore, we determined that UO and DO were classified as the ores.

However, the properties of DO were much lower than those of UO in Figures 4 and 5. Additionally, the metallic contents (iron, titanium, and vanaduim) in DO1-1 were obviously small compared to those of UO9 in Figure 8. Thus, we considered that the ore minerals in UO were more abundant than those of DO.

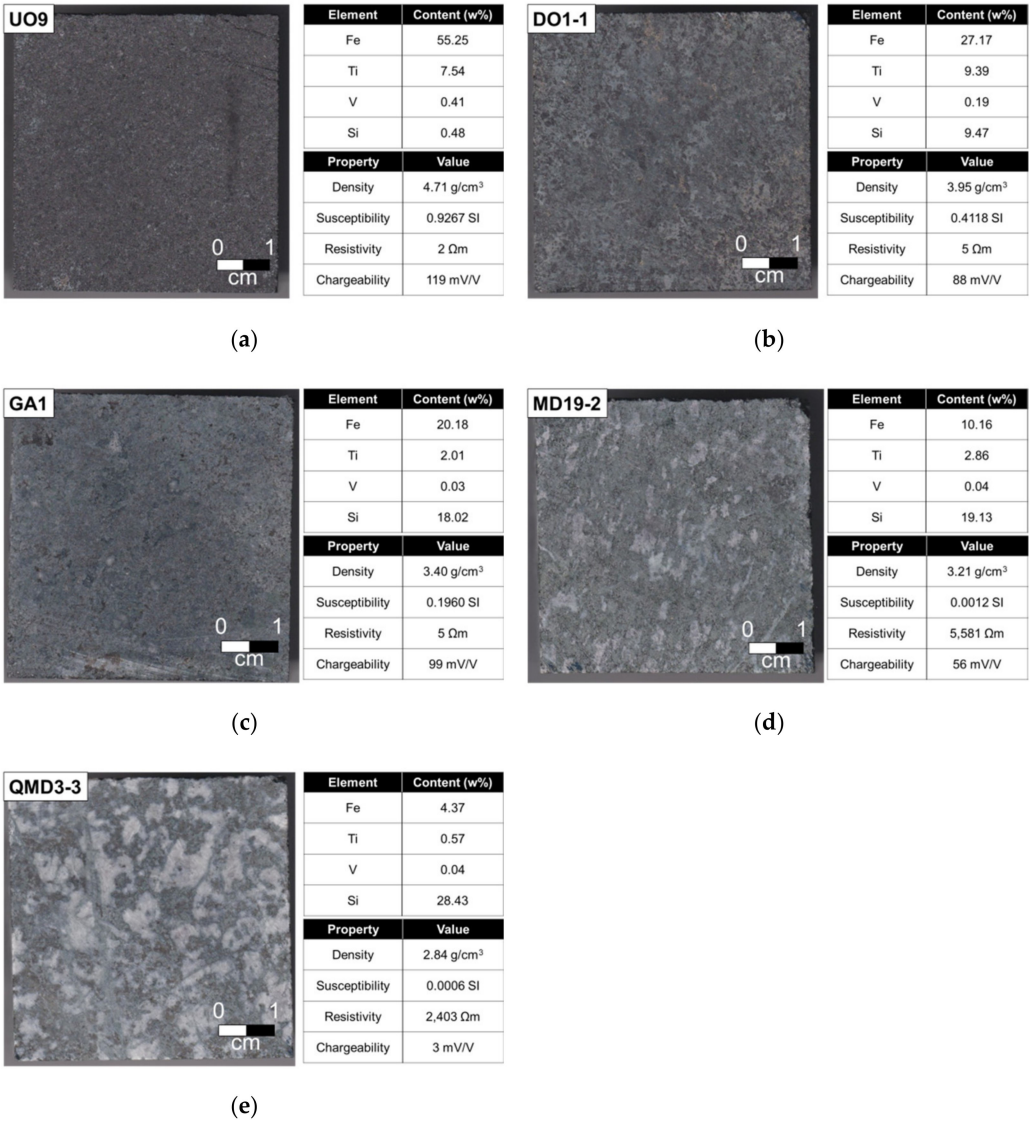

Figure 8. Rock slabs images, potable X-ray fluorescence analysis results, and geophysical properties of five kinds of rock samples showing (**a**) underground ore, (**b**) discovered ore, (**c**) gabbro, (**d**) monzodiorite, and (**e**) quartz monzodiorite.

The properties of GA were higher than gabbro [17]. The ranges of the properties were involved in those of magnetite gabbro [14]. Moreover, there is a considerable overlap of the properties between GA and DO in Figures 4 and 5. Moreover, the metallic contents of GA1 were higher than those of MD19-2 and QMD3-3 in Figure 8. It was considered that the ore minerals in GA were more than MD, QMD, and the common gabbro. In order to compare the contents of the ore minerals, more geochemical data are required.

4. Conclusions

We retrieved and characterized the geophysical properties of rock samples in the Gonamsan intrusion (Korea) using data from laboratory experiments. All geophysical properties depend on the quantity of ore minerals. We provided the geophysical criteria to identify the boundaries between the hidden orebody and host rocks in the geophysical surveys. Geophysical criteria in terms of both density and susceptibility were more salient than those in terms of electrical properties. Both gravity and magnetic surveys have been shown to be effective for mineral exploration in VTM deposits. The vertical resolution of gravity and magnetic surveys is physically far lower than that of electrical/electromagnetic

surveys. Thus, we can execute an effective mineral exploration in the VTM deposits by integrating multiple geophysical data using our geophysical characterization of the rocks.

Author Contributions: Conceptualization, S.S.; methodology, S.S.; software, S.S.; validation, E.K., J.L. and S.C.; formal analysis, S.S.; investigation, S.S., E.K. and J.L.; resources, S.S.; data curation, S.S.; writing—original draft preparation, S.S.; writing—review and editing, E.K. and J.L.; visualization, S.S.; supervision, S.C.; project administration, S.C.; funding acquisition, S.C. All authors have read and agreed to the published version of the manuscript.

Funding: This research was supported by the Basic Research Project (GP2020-007) of the Korea Institute of Geoscience and Mineral Resources (KIGAM) funded by the Ministry of Science and ICT (MIST), Korea.

Data Availability Statement: Not applicable.

Acknowledgments: We appreciate anonymous reviewers for the insightful comments.

Conflicts of Interest: The authors declare no conflict of interest.

References

1. Lee, B.Y.; Oh, C.W.; Lee, S.H.; Seo, J.; Yi, K. Ages and tectonic settings of the neoproterozoic igneous rocks in the gyeonggi massif of the southern Korean peninsula and the correlation with the neoproterozoic igneous rocks in China. *Lithos* **2020**, *370–371*, 105625. [CrossRef]
2. Schulz, K.J.; DeYoung, J.H.; Seal, R.R.; Bradley, D.C. *Critical Mineral Resources of the United States: Economic and Environmental Geology and Prospects for Future Supply*; United States Geological Survey: Washington, DC, USA, 2018.
3. Aramendia, I.; Fernandez-Gamiz, U.; Martinez-San-Vicente, A.; Zulueta, E.; Lopez-Guede, J.M. Vanadium redox flow batteries: A review oriented to fluid-dynamic optimization. *Energies* **2021**, *14*, 176. [CrossRef]
4. Arndt, N.; Fontboté, L.; Hedenquist, J.; Kesler, S.E.; Thompson, J.F.; Wood, D.G. Future global mineral resources. *Geochem. Perspect.* **2017**, *6*, 1–171. [CrossRef]
5. Kim, B.; Jeong, S.; Bang, E.; Shin, S.; Cho, S. Investigation of iron ore mineral distribution using aero-magnetic exploration techniques: Case study at Pocheon, Korea. *Minerals* **2021**, *11*, 665. [CrossRef]
6. Shin, Y.; Shin, S.; Cho, S.-J.; Son, J.-S. Application of 3D electrical resistivity tomography in the Yeoncheon titanomagnetite deposit, Korea. *Minerals* **2021**, *11*, 563. [CrossRef]
7. Kee, W.; Lim, S.; Kim, H.; Kim, B.; Hwang, S.; Song, K.; Kim, Y. *Geological Report of the Yeoncheon Sheet (1:50,000)*; Korea Institute of Geoscience and Mineral Resources (KIGAM): Daejeon, Korea, 2008.
8. Lee, J. *Iron-Ti (-V) Oxide Mineralization Related to Magmatic Fractionation of the Gonamsan Intrusion in Pocheon, South Korea*; Konju National University: Gongju, Korea, 2021.
9. Telford, W.M.; Telford, W.M.; Geldart, L.P.; Sheriff, R.E. *Applied Geophysics*; Cambridge University Press: Cambridge, UK, 1990.
10. Bieniawski, Z.T.; Bernede, M.J. Suggested methods for determining the uniaxial compressive strength and deformability of rock materials: Part 1. Suggested method for determining deformability of rock materials in uniaxial compression. *Int. J. Rock Mech. Min. Sci. Geomech. Abstr.* **1979**, *16*, 138–140. [CrossRef]
11. Archie, G.E. The electrical resistivity log as an aid in determining some reservoir characteristics. Petroleum development and technology. *Proc. Amer. Inst. Min. Met. Eng.* **1942**, *146*, 54–62.
12. Shin, S.W.; Park, S.; Shin, D.B. Spectral-induced polarization characterization of rocks from the Handuk iron mine, South Korea. *Environ. Earth Sci.* **2016**, *75*, 827. [CrossRef]
13. Han, M.-H.; Shin, S.W.; Park, S.; Cho, S.-J.; Kim, J.-H. Induced polarization imaging applied to exploration for low-sulfidation epithermal au–ag deposits, Seongsan mineralized district, South Korea. *J. Geophys. Eng.* **2016**, *13*, 817. [CrossRef]
14. Ashwal, L.D.; Webb, S.J.; Knoper, M.W. Magmatic stratigraphy in the bushveld northern lobe: Continuous geophysical and mineralogical data from the 2950 m bellevue drillcore. *S. Afr. J. Geol.* **2005**, *108*, 199–232. [CrossRef]
15. Xue, Y.; Jing, L.; Song, T. A study of taihe iron deposit in sichuan, china based on magnetic anomalies. In Proceedings of the International Geophysical Conference, Qingdao, China, 17–20 April 2017; pp. 477–480.
16. Lawton, D.C.; Hochstein, M.P. Physical properties of titanomagnetite sands. *Geophysics* **1980**, *45*, 394–402. [CrossRef]
17. Hunt, C.P.; Moskowitz, B.M.; Banerjee, S.K. Magnetic properties of rocks and minerals. *Rock Phys. Phase Relat.* **1995**, *3*, 189–204.